DNA Repair 83 (2019) 102720

Contents lists available at ScienceDirect

DNA Repair

journal homepage: www.elsevier.com/locate/dnarepair

The roles of fission yeast exonuclease 5 in nuclear and mitochondrial genome stability

Justin L. Sparks[a,b], Kimberly J. Gerik[a], Carrie M. Stith[a], Bonita L. Yoder[a], Peter M. Burgers[a,*]

[a] Department of Biochemistry and Molecular Biophysics, Washington University School of Medicine, St. Louis, MO 63110, USA
[b] Department of Biological Chemistry and Molecular Pharmacology, Harvard Medical School, Boston, MA 02115, USA

ARTICLE INFO

Keywords:
Exo5
Exonuclease
Fission yeast
Mitochondrial replication
Interstrand crosslink repair

ABSTRACT

The Exo5 family consists of bi-directional, single-stranded DNA-specific exonucleases that contain an iron-sulfur cluster as a structural motif and have multiple roles in DNA metabolism. *S. cerevisiae* Exo5 is essential for mitochondrial genome maintenance, while the human ortholog is important for nuclear genome stability and DNA repair. Here, we identify the Exo5 ortholog in *Schizosaccharomyes pombe* (spExo5). The activity of spExo5 is highly similar to that of the human enzyme. When the single-stranded DNA is coated with single-stranded DNA binding protein RPA, spExo5 become a 5′-specific exonuclease. *Exo5Δ* mutants are sensitive to various DNA damaging agents, particularly interstrand crosslinking agents. An epistasis analysis places *exo5*$^{+}$ in the Fanconi pathway for interstrand crosslink repair. *Exo5*$^{+}$ is in a redundant pathway with *rad2*$^{+}$, which encodes the flap endonuclease FEN1, for mitochondrial genome maintenance. Deletion of both genes lead to severe depletion of the mitochondrial genome, and defects in respiration, indicating that either spExo5 or spFEN1 is necessary for mitochondrial DNA metabolism.

1. Introduction

Exonuclease 5 (Exo5) was discovered in the 1980s in a biochemical screen for exonucleases in *S. cerevisiae* [1]. However, the catalytic activities and cellular functions of the enzyme were only recently analyzed, initially in *S. cerevisiae*, and subsequently in mammals [2,3]. Both Exo5 orthologs are bi-directional, single-stranded DNA (ssDNA)-specific exonucleases. Human Exo5 (hExo5) slides along ssDNA prior to cleavage, generating products that are varying in size [3], whereas *S. cerevisiae* Exo5 (scExo5) preferentially cleaves dinucleotides as its major product [2].

A phylogenetic analysis of Exo5 shows a wide-spread occurrence of the enzyme, including fungi, plants and mammals. But not all species have an Exo5. This includes some well-studied model organisms. The enzyme is apparently missing from all insects and from nematodes, but not from the *Priapulida* worms. It is also missing from all birds, except for the small *Palaeognathae* superorder, which contains Emu and Ostrich (Supplementary Fig. S1). Therefore, it appears that Exo5 was lost on multiple occasions during evolution. In addition, there also is an apparent divergence in cellular function in different organisms. All members of the *Saccharomycetales* order of fungi show a strong mitochondrial localization sequence for Exo5, and indeed the *S. cerevisiae EXO5* deletion is defective for mitochondrial DNA maintenance, but shows no apparent nuclear genome stability defect [2]. However, most orthologs outside the *Saccharomycetales* order lack a mitochondrial localization sequence, indicating that their main function may be nuclear (Supplementary Fig. S1). Accordingly, studies of the human Exo5 ortholog revealed it to be a protein with both cytoplasmic and nuclear localization, which is important for nuclear genome stability and DNA repair [3].

Mutations in the nuclease domain of human EXO5 are associated with testicular cancer and several other cancers [4]. However, such cases are infrequent in the cancer genome atlas (portal.gdc.cancer.gov). Much more common is the very high frequency of EXO5 silencing in many cancer types including glioblastoma (46%) and stomach adenocarcinomas (57%), such that EXO5 silencing makes up 95% of all EXO5 alterations [5].

Given the importance of EXO5 as a putative tumor suppressor, we were interested in a genetically more tractable model system to investigate the *in vivo* functions of Exo5 outside of the *Saccharomycetales* order, in order to better understand the nuclear functions of Exo5. The fission yeast *Schizosaccharomyces pombe* is an attractive model organism, particularly since a large-scale proteomic study indicated that *S. pombe* Exo5 (spExo5) is localized to both the nucleus and mitochondrion [6].

In this paper we describe the biochemical and genetic

* Corresponding author.
E-mail address: burgers@wustl.edu (P.M. Burgers).

https://doi.org/10.1016/j.dnarep.2019.102720
Received 7 May 2019; Received in revised form 4 September 2019; Accepted 19 September 2019
Available online 21 September 2019

characterization of spExo5. We observed that spExo5 is a bi-directional, ssDNA-specific exonuclease that shows a strikingly similar cleavage specificity to the previously characterized mammalian orthologs. Like with human Exo5, coating of the ssDNA with RPA restricts the activity of spExo5 to that with a unique 5′-3′ directionality. Fission yeast *exo5Δ* strains are sensitive to UV-irradiation, to alkylating agents, and in particular to interstrand crosslinking (ICL) agents. These results closely recapitulate our previous Exo5 knockdown experiment in human cells [3]. Finally, we demonstrate that spExo5 plays a redundant role with the flap endonuclease FEN1 (*rad2*$^+$ in *S. pombe*), for the maintenance of mitochondrial DNA. Remarkably, an *exo5Δ rad2Δ* double deletion strain shows a severe decrease in mitochondrial DNA copy number and an associated defect in respiratory growth.

2. Materials and methods

2.1. Materials and reagents

DNA modification and restriction enzymes were from New England Biolabs (Ipswich, MA). The drugs used were all from Sigma-Aldrich (St. Louis, MO): cis-platin (diammine*cis*-platinum(II) dichloride), cat. no. P4394; methyl methanesufonate (MMS), cat. no. 129925; 8-MOP (8-methoxypsoralen), cat. no. M3501. Monoclonal anti-humanPCNA antibody PC10 was purchased from Santa Cruz Biotechnology and used to probe for *S. pombe* PCNA as described [7]. Oligonucleotides were purchased from IDT (Coralville, IA) and purified by urea-polyacrylamide gel electrophoresis (PAGE): c81, TTGCCGATGAACTTTTTTTTT TGATC GAGACCTT; v81 AAGGTCTCCATCAAAAAAAAAAGTTCATCGGCAA. The polarity switch oligonucleotides were a gift from Tim Lohman of this Department. The 5′-^{32}P-label was introduced on oligonucleotides c81 or 5′-5′ polarity switch oligonucleotide using [γ-^{32}P] ATP and T4 Polynucleotide kinase. The 3′-^{32}P-label was added to 3′-3′ polarity switch oligonucleotide by incubation with [α-^{32}P] dATP with terminal deoxynucleotide transferase under manufacturers' conditions.

2.2. S. pombe strains

The *exo5Δ* strain was obtained from Bioneer Corporation. Double disruption mutants were either obtained by crossing the *exo5Δ* strain with strains containing other repair gene disruptions, or by direct integration of deletion marker cassettes. Genotypes of the double deletion strains were confirmed by diagnostic PCR. Strains are listed in Supplementary Table 1.

Growth of strains containing *Exo*$^+$ plasmids was carried out on EMM media lacking Leu or Ura as appropriate, containing 5 μM thiamine (non-inducing conditions), or as otherwise indicated.

2.3. Plasmids

Plasmid pBL281 (*S. pombe*) contains the *Schistosoma japonicum* glutathione S-transferase (GST) gene fused to the N terminus of the Exo5 gene in vector pRS424-GALGST [8]. The GST tag is separated from the N terminus of the *S. pombe,* human, and mouse Exo5 gene by a recognition sequence for the human rhinoviral 3C protease (LEVLFQ/GP). Following cleavage by the protease, the N-terminal sequence of *S. pombe* Exo5 is extended with the GPEF sequence. Plasmid pBL281-207 has an active site mutation D207. Plasmid pBL281-176 has an active site mutation D176A. *S. pombe* expression plasmids pREP3x-spExo5 has spExo5 under the control of the repressible *nmt* (no message in thiamine) promoter. Plasmids and sequences are available upon request. The pBL288 plasmid series has the *Exo5*$^+$ cDNA (or mutants) cloned into plasmid pREP3X (*ars1 Leu2+ nmt* promoter and terminator) under control of the repressible *nmt* promoter. The pBL289 series has a triple FLAG tag fused to the C-terminus of the *Exo5*$^+$ cDNA (or mutants) in the pBL288 plasmid backbone. The pBL298 series has GFP fused to the C-terminus of the *Exo5*$^+$ cDNA (or mutants) in vector pREP4X (*ars1 Ura4*$^+$ *nmt* promoter and terminator) under control of the repressible *nmt* promoter.

Oligonucleotides were purchased from IDT (Coralville, IA) and purified by urea-polyacrylamide gel electrophoresis (PAGE): c81, TTG CCGATGAACTTTTTTTTT TGATCGAGACCTT; v81 AAGGTCTCCATCA AAAAAAAAAGTTCATCGGCAA. The polarity switch oligonucleotides were a gift from Tim Lohman of this Department. The 5′-^{32}P-label was introduced on oligonucleotides c81 or 5′-5′ polarity switch oligonucleotide using [γ-^{32}P] ATP and T4 Polynucleotide kinase. While the 3′-^{32}P-label was added to 3′-3′ polarity switch oligonucleotide by incubation with [α-^{32}P] dATP with terminal deoxynucleotide transferase under manufacturers' conditions.

2.4. Exo5 overproduction and purification

Overproduction was carried out in *S. cerevisiae* strain FM113 (MAT**a** *ura-3-52 trp1-289 leu2-3112 prb1-1122 prc1-407 pep4-3*) transformed with plasmid pBL281 (*S. pombe* Exo5), pBL281-207 (*S. pombe* Exo5-D207A), or pBL281-176 (*S. pombe* Exo5-D176). Growth, induction, and extraction were similar to the procedures described previously [9]. Cells were harvested and resuspended in 1/2 the volume of 3x buffer A (buffer A: 60 mM HEPES-NaOH [pH 7.8], 0.4 M sodium acetate, 0.1 mM EDTA, 0.01% polyoxyethylene (10) lauryl ether, 10 mM sodium bisulfite, 10 μM pepstatin A, 10 μM leupeptin), then frozen in liquid nitrogen. The frozen cell pellets were then blended in dry ice powder. All further preparation was carried out at 0–4 °C. After the thawing of the lysate, 10% glycerol, 1 mM dithiothreitol (DTT), 0.05 mM phenylmethylsufonyl fluoride (100 mM stock), and 150 mM ammonium sulfate (4 M stock), 0.45% polymin P (10% stock, pH 7.3) were added to the lysate. The mixture was stirred for 15 min, the lysate was cleared at 40,000 × g for 30 min, and the supernatant was precipitated with 0.31 g/ml solid ammonium sulfate. The precipitate was collected at 40,000 × g for 30 min and then redissolved in buffer A_0 (subscript indicates the sodium acetate concentration) 10% glycerol, and 1 mM dithiothreitol until the lysate conductivity was equal to that of buffer A_{400}. The lysate was then used for batch binding to 1 ml of glutathione-Sepharose 4B beads (GE Healthcare), equilibrated with buffer A_{400}, and gently rotated at 4 °C for two hours. GST-beads were collected at 1000 rpm in a swinging-bucket rotor, followed by batch washes (3 × 20 ml of buffer A_{400}). The beads were transferred to a 10 ml column and washed at 2.5 ml/min with 100 ml of buffer A_{400}. The second washing was with 50 ml buffer A_{400} containing 5 mM Mg-acetate and 1 mM ATP. And the third washing used 50 ml of buffer A_{400} and 30 ml of buffer A_{200}. Elution was carried out with a flow rate of 0.2 ml/min with buffer A_{200} containing 20 mM glutathione (pH adjusted to 8.0). The protein was eluted into four fractions. The fractions containing pure protein were incubated over night at 4 °C with 30U of rhinoviral 3C protease, diluted with A_0 to equal A_{100} and loaded on a 1-ml Mono Q column. Protein was eluted with a linear gradient of buffer A_{100} to A_{1200}. Pure Exo5 protein was eluted at 300 mM–400 mM sodium acetate. Exo5 mutants were purified similarly throughout the procedures described.

2.5. SpExo5 co-immunoprecipitation

Co-IPs were carried out in *S. pombe* strain PYP102 (*exo5Δ*) by transformation of pBL289 or mutant. Cells were grown in Edinburgh minimal media (EMM) supplemented with 5 μM thiamine overnight. Cells were then harvested and resuspended in 1/2 the volume of 3x buffer A (buffer A: 60 mM HEPES-NaOH [pH 7.8], 150 mM sodium chloride, 0.1 mM EDTA, 0.05% polyoxyethylene (10) lauryl ether, 10 mM sodium bisulfite, 10 μM pepstatin A, 10 μM leupeptin), then frozen in liquid nitrogen. The frozen cell pellets were then blended in dry ice powder. All further preparation was carried out at 0–4 °C. After the thawing of the lysate, 10% glycerol, 1 mM dithiothreitol (DTT), and 0.5 mM phenylmethylsufonyl fluoride (100 mM stock) were added to

the lysates. The lysates were cleared at 40,000 × g for 30 min, and the cleared lysate was then used for batch binding to FLAG-M2-beads (SIGMA), equilibrated with buffer A_{150}, and gently rotated at 4 °C for two hours. FLAG-M2-beads were collected at 1000 rpm in a swinging-bucket rotor, followed by batch washes (3 × 500 µl of buffer A_{150}). The second washing was with 500 µl buffer A_{150} containing 5 mM Mg-acetate and 1 mM ATP. And the third washing used (3 × 500 µl of buffer A_{150}). Elution was carried out in buffer A_{150} containing 150 µg/ml 3XFLAG peptide (SIGMA). The protein was eluted into two fractions and analyzed by SDS-PAGE followed by coomassie brilliant blue staining.

2.6. Exonuclease assays

The standard 10 µl assay mixture contains 100 mM Tris-HCl (pH 7.8), 500 µg/ml bovine serum albumin, 5 mM DTT, 5 mM Mg-acetate, 50 mM NaCl, 50–100 fmol of ^{32}P-end-labeled oligonucleotide substrate, and enzyme. Incubations were carried out at 30 °C for the indicated time periods. Deviations from the standard assay conditions are indicated in the legends of the figures. Reactions were stopped with 10 mM final concentration of EDTA in addition to 40% formamide and analyzed on a 17% PAGE-7 M urea electrophoresis. After the gels were dried, they were subjected to phosphorimager analysis.

2.7. S. pombe damage sensitivity assays

Strains were inoculated in 5 ml of liquid yeast extract supplemented (YES) medium and grown overnight at 30 °C with shaking. The cells were then washed in phosphate-buffered saline and the cell density was determined by spectroscopy at 595 nm. Serial 10-fold dilutions of late-log-phase cells, from 10^5 to 10 cells per spot, were spotted onto YES plates or YES plates containing the indicated concentrations of cis-platin (mM) or methyl methanesulfonate (MMS, %). Other YES plates were irradiated with the indicated dose of UV254 (J/m^2) or ionizing radiation (Gy). For 8-methoxypsoralen treatment cells were grown to an OD of 0.4 and then treated with 5 µg/ml 8-methoxypsoralen for 15 min at 30 °C, followed by no irradiation (-), or irradiation at 365 nm with the indicated dose to activate the psoralen crosslinks. Cells were washed twice with PBS buffer and diluted for spotting on YES plates. Plates were grown for 2–3 days at 30 °C and photographed.

3. Results and discussion

3.1. Fission yeast and human Exo5 have comparable structures and activities

Budding yeast and human Exo5 show a conserved arrangement of cysteine residues that is also conserved in the nuclease domain of the *B. subtilis* AddAB recombinase and the Dna2 nuclease-helicase (Fig. 1A). These enzymes contain an iron-sulfur cluster moiety that is dependent on the presence of these cysteines [3,10,11]. Cys-Ser mutations in hExo5 resulted in a loss of iron-sulfur occupancy and an associated large decrease in enzymatic activity [3]. The conserved quartet of cysteine residues extends to fission yeast Exo5 (Fig. 1A). We over-expressed and affinity-purified spExo5 from *S. cerevisiae* (Materials and Methods). The purified enzyme shows an absorption at 410 nm, characteristic of a [4Fe-4S] iron-sulfur cluster (Fig. 1B,C).

We next investigated the enzymatic properties of spExo5 with the purpose of determining whether they were more like that of the *S. cerevisiae* or the human enzyme. The Exo5 family shows a strong conservation of active site residues (Fig. 1A). Mutation of either of two conserved aspartates that chelate the divalent metal required for catalysis resulted in a complete abrogation of enzymatic activity *in vitro* and a null phenotype *in vivo* for the budding yeast and the human enzymes [2,3]. Consistent with these studies, mutation of either of the analogous active site aspartates to alanines (D176A, D207A), abrogated the nuclease activity of spExo5 (Supplementary Fig. S2A).

The Exo5 enzymes are designated as ssDNA-specific exonucleases due to their inability to degrade double-stranded DNA or circular ssDNA, i.e. they need an end as loading site [2,3]. SpExo5 shares these properties with the budding yeast and mammalian family members. The enzyme is inactive on circular ssDNA (not shown) and on dsDNA (Fig. 1F). However, while budding yeast Exo5 generates predominantly dinucleotides as digestion products from a linear ssDNA substrate, both human and fission yeast Exo5 generate a large range of oligonucleotides (Fig. 1D). A comparison of the cleavage pattern generated by spExo5 with that by hExo5 revealed a remarkable similarity, with both enzymes exhibiting a dominant cleavage site that yielded a 10-mer. The two likely interpretations of that result are that either spExo5 prefers cutting at a distance ten nucleotides from the 5′-end, or that the ten-mer product results from preferential sequence or structure context. Cleavage of hompolymeric $(dT)_{65}$ was entirely random (Fig. 1G, Supplementary Fig. S2B), which does not support the distance measuring model. Our interpretation of these data is that both forms of Exo5 load at one end and carry out a random walk along the ssDNA substrate prior to cutting, hence the name sliding exonuclease. However, despite the remarkable similarity in cleavage pattern (Fig. 1D), spExo5 is a much more active enzyme. At saturating DNA concentrations, the turnover number for spExo5 was about 100-fold higher than that of hExo5, 1 s^{-1} vs 0.012 s^{-1}, respectively (Fig. 1E). An important caveat inherent to this comparison is that human Exo5 may require an as yet unidentified cofactor that stimulates its catalytic activity.

We next investigated the directionality of exonuclease action and the role of RPA in mediating directionality. The cleavage pattern observed in Fig. 1D could result from the enzyme loading at either the 5′- or 3′-terminus, followed by sliding along ssDNA prior to cleavage. The data in Fig. 1F suggest that spExo5 can load at either the 5′- or 3′-end. When the 3′-end was made inaccessible for Exo5 loading by hybridizing a complementary 14-mer (lanes 9–11), the cleavage pattern was similar to that of the ssDNA substrate. However, when the 5′-end was similarly made inaccessible (lanes 12–14), longer-sized products were generated, consistent with 3′-loading. Based on the disappearance of the 34-mer with increasing enzyme concentrations, the data also indicate that 5′-loading is more efficient than 3′-loading, by a factor of about five. An analysis of the activity of spExo5 on reverse polarity oligonucleotides is consistent with these conclusions (Supplementary Fig. S2B). The reverse polarity oligo$(dT)_{70}$ substrates contain a polarity reversal in the middle, either a 3′-3′ or 5′-5′ internucleotide linkage, such that the two ends of the oligo(dT) have either two 5′-ends or two 3′-ends, respectively. Similar to previously determined for the human enzyme [3], spExo5 showed activity on either substrate, with a preference for the 5′-ended substrate (Supplementary Fig. S2B).

In a physiologically relevant setting, ssDNA is normally coated with the ssDNA binding protein RPA. Both human Exo5 and the structurally related Dna2 nuclease assume a unique 5′-directionality when the ssDNA is coated with RPA [3,12]. Likewise, coating of 5′-labeled $(dT)_{65}$ with increasing concentrations of either human or *S. cerevisiae* RPA yielded progressively smaller oligonucleotides as products, which we propose to originate from 5′-loading and cutting near the 5′-end (Fig. 1G). Importantly, no products were seen in which the length of $(dT)_{65}$ was reduced by just a few nucleotides, which would have been indicative of 3′-loading and cutting near the 3′-end. From these experiments we conclude that spExo5 shows remarkably similar enzymatic properties to hExo5 with regard to substrate cleavage specificities. The major difference is its increased catalytic efficiency. Therefore, we propose that *S. pombe* may be a tractable model system for understanding mammalian Exo5 function.

3.2. Mitochondrial and nuclear localization of spExo5

The genome stability and DNA damage phenotypes of a *S. cerevisiae EXO5* deletion mutant are fully consistent with the sole mitochondrial

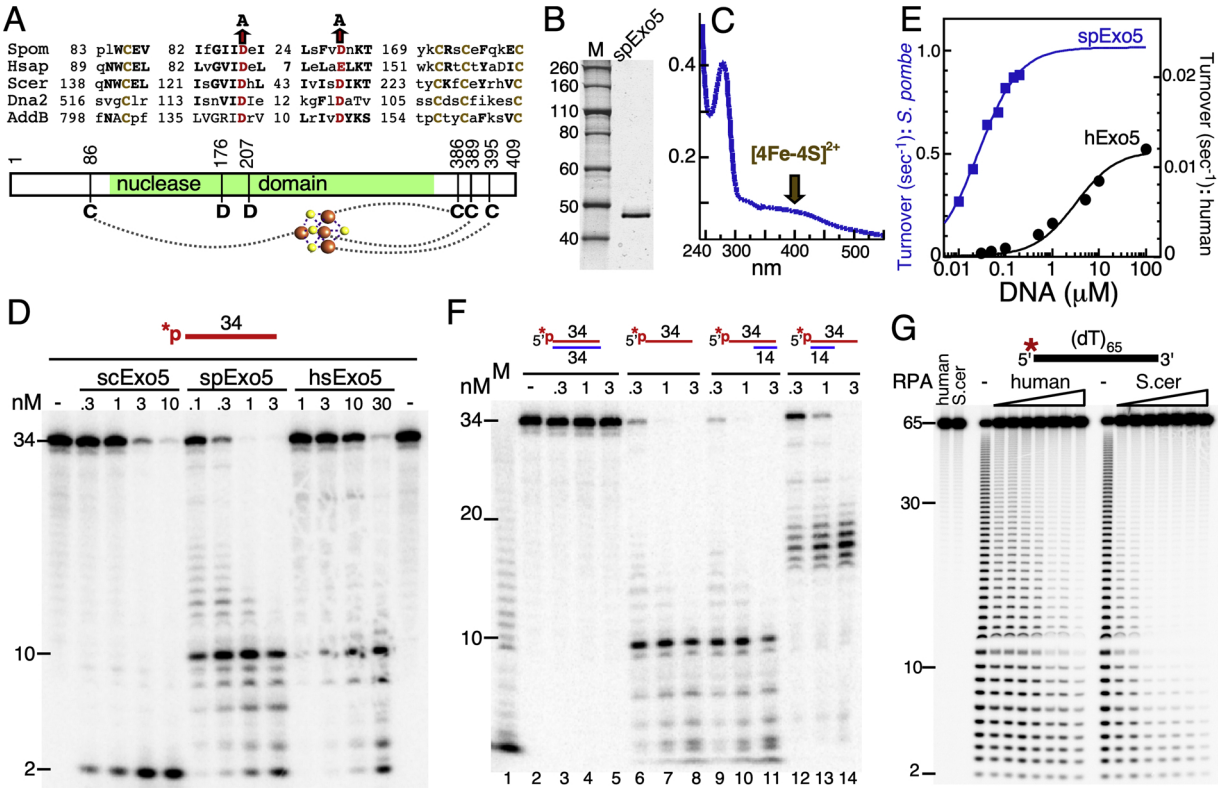

Fig. 1. Biochemical activities of spExo5. (A) Conserved sequence motifs in the Exo5 family. Brown, cysteines that ligand the Fe-S cluster; red, catalytic residues. (B) 12% SDS-PAGE of purified spExo5. Staining was with Coomassie. (C) UV spectrum of purified spExo5; Absorption at 410 nm is indicative of the presence of a Fe-S cluster. (D) Comparison of activities of *S. cerevisiae*, *S. pombe*, and human Exo5 on a 34-nucleotide oligonucleotide. Standard assays contained 10 nM 5′-^{32}P-labeled ssDNA substrate at the indicated concentrations of scExo5, spExo5, or hsExo5 for 4 min at 30 °C. Samples were analyzed on a 7 M urea-17% polyacrylamide gel. (E) Dependence of hExo5 and spExo5 activity on the concentration of 34-mer ssDNA. Data were fit to a Michaelis-Menten model. For spExo5, Km = 26 ± 2.2 nM and Vmax = 1 ± 0.2 s^{-1}; for hExo5, Km = 3200 ± 800 nM and Vmax = 0.012 ± 0.002 s^{-1}. (F) Standard assays on 10 nM of the indicated fully dsDNA (lanes 2–5), ssDNA (lanes 6–8) and partial dsDNA (lanes 9–14) substrates, with indicated concentrations of spExo5. M, ladder from partial digestion of ssDNA with snake venom phosphodiesterase, a 3′-exonuclease. (G) 5′-directionality of spExo5 enforced by human or *S. cerevisiae* RPA. Standard assay mixtures used 10 nM 5′-^{32}P-labeled $(dT)_{65}$ substrate and 0.15 nM spExo5 with either no RPA, or 10, 12.5, 15, 20, 25, 30, or 40 nM of the indicated RPA for 5 min at 30 °C. Lanes 1 and 2 were control assays without Exo5 and with 40 nM of the indicated RPA.

localization of the protein [2]. On the other hand, depletion of human Exo5 is associated with nuclear chromosome integrity defects, and these are enhanced when cells are subjected to stress [3]. Because our genetic studies, to be described below, suggested the presence of both nuclear and mitochondrial defects in *exo5* mutants, we have investigated the localization of Exo5 in more detail. A previous proteomic localization study already indicated that the protein was localized to both the nucleus and the mitochondrion [6]. However, a putative N-terminal localization signal for mitochondrial import is lacking (Supplementary Fig. S1; probability = 0.00), using the Predotar prediction algorithm (https://urgi.versailles.inra.fr/Tools/Predotar). Nevertheless, mitochondrial localization might be mediated by another mechanism(s). *S. pombe* Exo5 contains several internal methionines in the unstructured ~80 amino acid long N-terminal region prior to the nuclease catalytic core. Alternative start site usage to direct subcellular localization is not an unusual mechanism. Human FEN1 has an alternative translation start site leading to a short, functional isoform that localizes to mitochondria, whereas the full-length form localizes to the nucleus [13]. Similarly, the nuclear and mitochondrial isoforms of the *S. pombe* Pif1 helicase result from alternative translation start sites [14]. Translation initiation at the Exo5-Met58 position was predicted by Predotar to have a mitochondrial localization probability of 0.18. Interestingly, Exo5 from two other *Schizosaccharomyces* species showed an even higher mitochondrial probability (0.6, 0.66) if initiation started at the analogous internal methionine. Therefore, we expressed in fission yeast three forms of Exo5: *Exo5*$^{+}$, *Exo5-M58A*, and *Exo5-Δ(1-57)*.

In order to carry out these experiments, *Exo5*$^{+}$ was fused to a C-terminal 3xFLAG tag, and cloned into a *S. pombe* expression plasmid under control of the thiamine-inducible *nmt* promoter (see Materials and Methods). The *nmt* promoter shows a basal level of Exo5-FLAG expression in the presence of high levels of thiamine (5 μM)[15]. However, expression is strongly induced when thiamine is omitted from the media (Supplementary Fig. S3A). Under these highly inducing conditions, Exo5-FLAG levels were increased dramatically, and cells carrying the *Exo5*$^{+}$ plasmid showed a negative growth phenotype (Supplementary Fig. S3B). The lethality phenotype resulting from Exo5 overexpression will be discussed in the next section. Addition to the growth media of 50 nM thiamine or higher was sufficient to relieve growth inhibition. At 50 nM thiamine, Exo5-FLAG levels are only slightly elevated from those at non-inducing conditions (Supplementary Fig. S3A). Therefore, all plasmid-based Exo5 studies (with or without C-terminal fusion tags or domains) were carried out with 5 μM thiamine in the media.

The affinity-purified wild-type Exo5-FLAG protein showed two prominent species by immunoblot blot analysis (Fig. 2A). The upper band is consistent with the predicted molecular weight of spExo5-3XFLAG protein (~50 kDa), while the lower band is consistent with that of a protein starting at Met58, followed by loss of a small signal peptide upon mitochondrial entry (~43 kDa). Importantly, the *M58A* mutant lacked the lower band, as one would expect if translation of the mitochondrial species started at Met58 with the M58A mutation eliminating this initiation. Conversely, the *Δ(1-57)* mutant showed only the

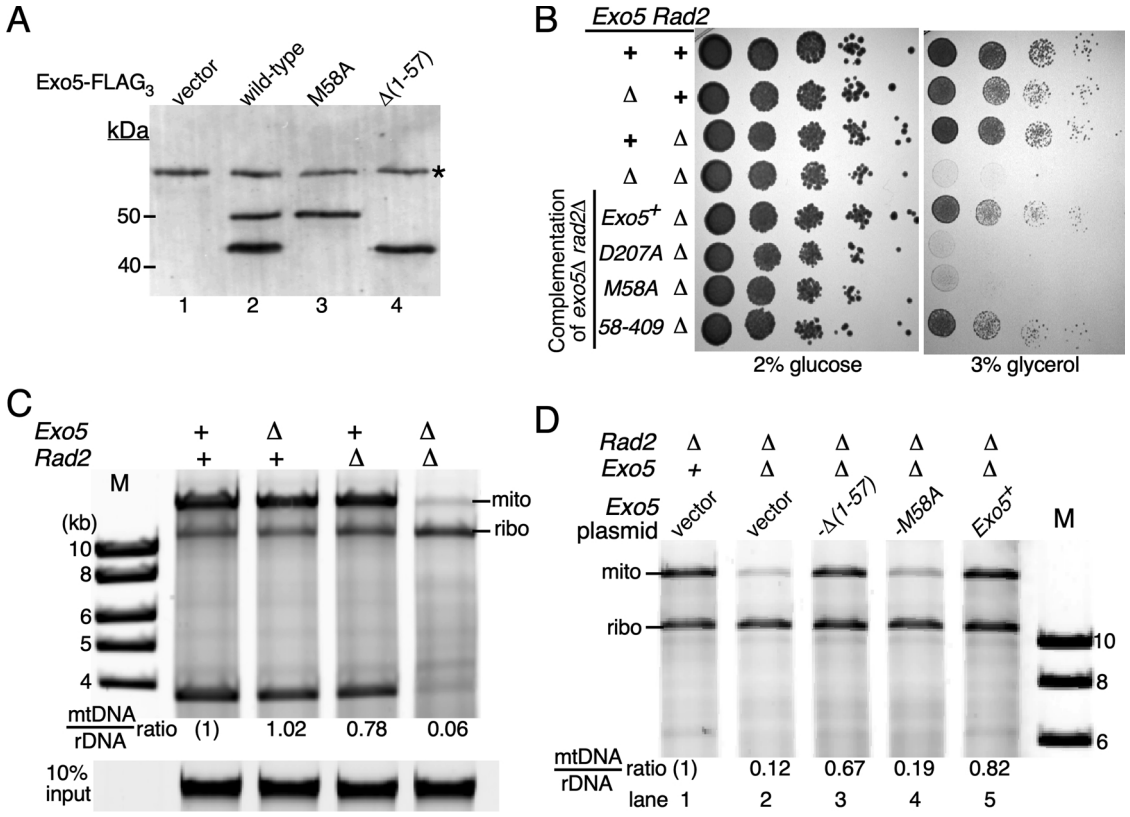

Fig. 2. Mitochondrial function of spExo5. (A) *Exo5Δ* strains containing the pBL289 (*exo5*$^{+}$-FLAG$_3$) series of plasmids, placed under control of the *nmt* promoter, or empty vector were grown under non-inducing conditions (5 μM thiamine), and extracts subjected to Western analysis with 3xFLAG antibodies. *, non-specific band. (B) Isogenic strains with the indicated *Rad2* or *Exo5* deletions, and the *Rad2Δ Exo5Δ* double mutant containing the pBL288 series of plasmids (last 4 entries), were grown on selective media (-Leu), and ten-fold serial dilutions plated on rich media with either glucose or glycerol. Growth was for 3 days (YES) or for 6 days (YEG) at 30 °C. (C) Isogenic strains with the indicated *Rad2* or *Exo5* deletions were grown on rich media and chromosomal DNA isolated and digested with restriction enzymes *Acl*I, *Age*I, *Pst*I, and *Pvu*II, and separated on a 1% agarose gel. Staining was with GelRed and the fluorescence was recorded with a Typhoon phosphoimager in the fluorescence mode. The enzyme mixture cuts chromosomal DNA into small fragments but cuts the ribosomal DNA array only once per repeat (10.8 kb) and the mtDNA twice (15.7 + 3.8). The ratio of the 15.7/10.8 bands was quantified, with that of wild-type set to (1). Bottom, 10% of undigested input DNA. (D) Plasmid containing strains from (B) were grown on selective media with 5 μM thiamine. Chromosomal DNA was isolated and restriction enzyme digested, and separated on a 0.7% agarose gel. Digestion and analysis was exactly as in (C).

lower band, further supporting our model.

We also expressed the same mutants with a C-terminal GFP tag under non-inducing conditions. Cells were fixed and observed by fluorescence microscopy. Wild-type *Exo5*$^{+}$ showed diffuse cytoplasmic fluorescence and both nuclear and punctate mitochondrial fluorescence. The *Exo5-M58A* mutant showed diffuse cytoplasmic/nuclear fluorescence, but lacked punctate fluorescence suggesting its exclusion from the mitochondria. The *Δ(1-57)* mutant showed only punctate staining suggesting that this truncated form of Exo5 is solely localized to the mitochondria (Supplementary Table 2). Therefore, both sets of data are consistent with a model in which mitochondrial localization of spExo5 proceeds through translational initiation at Met58, whereas initiation at Met1 yields predominantly the cytoplasmic and nuclear forms.

3.3. Exo5 interacts with RPA and PCNA

In order to potentially link spExo5 to specific DNA repair pathways, we performed co-immunoprecipitation experiments to find Exo5-interacting proteins (see Materials and Methods). Exo5-FLAG was expressed in a *exo5Δ* strain under non-inducing conditions. Cell extracts were subjected to co-immunopurification with 3xFLAG-beads and washed extensively prior to elution with a 3xFLAG peptide. The elutions were analyzed by SDS-PAGE followed by coomassie staining (Fig. 3A). While immunoprecipitation from the control extract showed very weak protein signals (lane 1), several proteins were easily detected after immunoprecipitation from the spExo5-3xFLAG-containing extract. The upper and lower sections of lane 2 (above and below the main spExo5 band) were cut out and analyzed by mass spectrometry. Mass finger printing identified several DNA replication and repair proteins with high significance. The full list of hits with high Mascot scores is in Supplementary Table 3. The top hits were two subunits of the single-stranded DNA binding protein RPA (Ssb1, Ssb2), two subunits of the 14-3-3 complex (Rad24, Rad25), and PCNA. Interestingly, the mitochondrial single-stranded DNA binding protein Rim1 was also identified as a significant hit, in accord with Exo5's mitochondrial localization (Supplementary Table 3). To further test some of these interactions, we obtained antibodies against the *S. pombe* RPA70 subunit (Ssb1) and PCNA (Pcn1) [7,16]. Indeed, both RPA and PCNA were detected by Western blot analysis in the Exo5-FLAG co-IPs, and not in the co-IPs from control extracts (Fig. 3B, Supplementary Fig. S3C). The interactions were not mediated through DNA as treatment with DNase I did not eliminate them (Fig. 3C, Supplementary Fig. S3D). Interestingly, co-IPs with the nuclease-defective form, *exo5-D207A*-FLAG, showed a strongly increased RPA and PCNA signal, suggesting that inactive Exo5-containg DNA repair complexes might be stalled on the DNA and therefore enriched during co-immunopurification (Fig. 3B). Previously, we showed biochemically that human Exo5 also interacts with human RPA [3]. The possible interaction of hExo5 with PCNA has not been investigated and neither form of Exo5 shows a PCNA consensus interaction (PIP) motif. The results from these experiments identify spExo5 through its interactions with both nuclear and mitochondrial

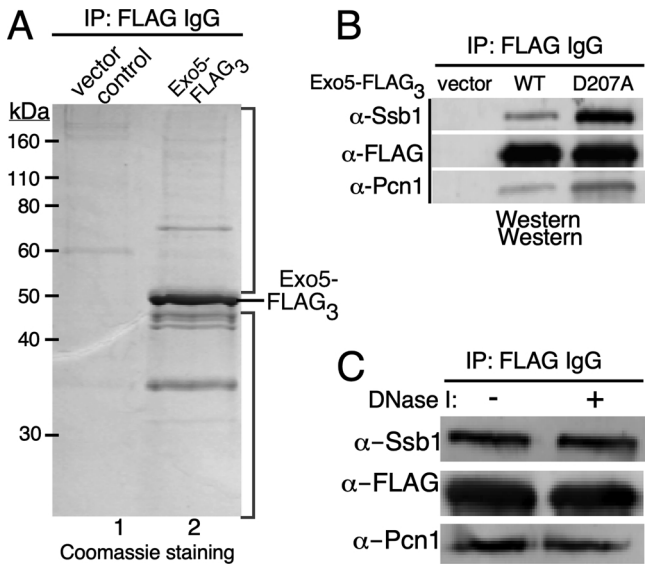

Fig. 3. SpExo5 interacts with spRPA and spPCNA. (A) Co-immunopurification with spExo5-FLAG$_3$ from *S. pombe* cells grown under low-expressive conditions (5 μM thiamine). Elutions from the 3xFLAG beads were analyzed on a 10%-SDS PAGE gel and stained with coomassie brilliant blue. (B) Immunoblot analysis of co-immunopurifications of extracts from *exo5Δ* cells containing either empty vector, or plasmids containing 3xFLAG-Exo5 or the nuclease-defective 3xFLAG-spExo5-D207A mutant. Antibodies used against 3xFLAG (spExo5-FLAG$_3$), spSsb1 (RPA70 subunit), and spPcn1 (PCNA). (C) Immunoblot analysis of extracts as in (B) either mock-treated or treated with DNaseI. The panels in (B) and (C) were assembled from the full Western blots shown in Supplementary Fig. S3C,D.

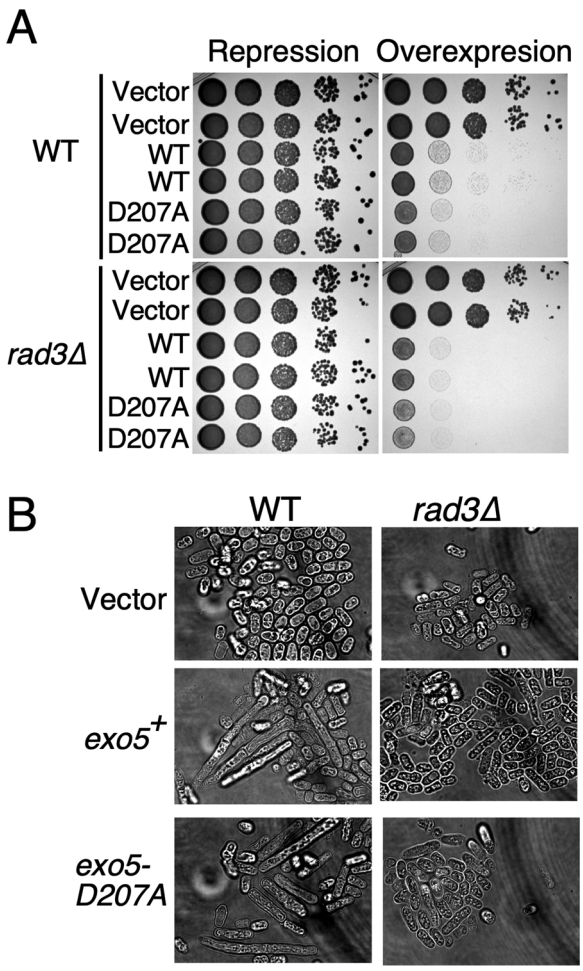

Fig. 4. Overexpression of SpExo5 causes checkpoint activation and cell death. (A) Overexpression of spExo5 leads to cell death in *S. pombe* cells regardless of checkpoint proficiency. Cells either WT or *rad3Δ* containing pREP3x-spExo5 or pREP3x-spExo5-D207A were grown overnight in EMM-leu supplemented with 5μM thiamine. Cells were washed serially diluted on plates either containing 15 μM or 0 μM thiamine and incubated 2–3 day at 30 °C. (B) Light microscopy of cells from (A), either grown on plates containing 15 μM or 0 μM thiamine for 2–3 days.

DNA metabolic factors, but further work is required to characterize the nature and significance of these various interactions.

During our spExo5 expression experiments, we noticed that overexpression of *Exo5*$^+$ from the strong *nmt* promoter in selective minimal media lacking thiamine caused lethality (Fig. 4A, Supplementary Fig. S3B). This lethality was not due to the nuclease activity of the protein, since overexpression of the nuclease-deficient mutant (*exo5-D207A*) showed similar lethality. Examination of the cell morphology revealed that the cells were elongated, indicative of checkpoint activation [17] (Fig. 4B). The DNA damage and replication checkpoints are mediated through activation of the Rad3 protein kinase, the ortholog of human ATR [17,18]. However, while overexpression of *exo5-D207A* in a *rad3Δ* background eliminated the cell elongation phenotype, it did not suppress lethality (Fig. 4A,B). We hypothesize that checkpoint activation and lethality are the result of the increased Exo5 concentrations titrating away an essential replication factor(s), e.g. RPA or PCNA, from performing its proper functions during replication, but this hypothesis needs further testing.

3.4. *S. pombe Exo5 and FEN1 play a redundant role in mitochondrial DNA maintenance*

S. pombe is a petite negative yeast, which requires a functional mitochondrial genome for growth [19]. In glycerol-containing media, cells depend on respiration for energy source, which requires a fully functional mitochondrial machinery. Therefore, unlike in budding yeast, in fission yeast neither genotypic petite mutants (mutation or deletion of the mitochondrial genome) nor phenotypic petite mutants (failure to grow on a non-fermentable carbon source such as glycerol) are generally found. *S. pombe exo5Δ* strains are viable, indicating that spExo5 is not essential for mitochondrial genome stability (Fig. 2B). However, Exo5 is not the only 5′-nuclease present in mitochondria. The 5′-flap endonuclease FEN1 has a demonstrated involvement in mitochondrial genome maintenance in *S. cerevisiae* [20] and in human cells [21]. Therefore, it is reasonable to assume that *S. pombe* FEN1 (*rad2*$^+$) fulfills a similar mitochondrial function. Interestingly, while neither the single *exo5Δ* nor *rad2Δ* mutant is associated with a detectable mitochondrial growth phenotype, the double mutant *exo5Δ rad2Δ* showed a failure to grow on media lacking a fermentable carbon source (Fig. 2B). The double mutant also showed a minor growth defect on rich media containing glucose (Fig. 5D). Exogenous expression of wild-type *exo5*$^+$ restored the growth of these strains on glycerol plates and this restoration required the nuclease activity of Exo5 (Fig. 2B). Remarkably, expression of the short isoform *exo5-(58-409)*, which shows mitochondrial localization, was able to restore growth of the *exo5Δ rad2Δ* mutant on glycerol plates, but expression of the *exo5-M58A* mutant, which eliminates translation of the short isoform, did not.

As an initial investigation into the mitochondrial defect of the *exo5Δ rad2Δ* double mutant, we isolated genomic DNA from an isogenic set of strains and digested the DNA with a set of restriction enzymes that allowed us to quantify the ratio of mitochondrial DNA to ribosomal repeat DNA (Fig. 2C). We observed a severe loss of mitochondrial DNA from the *exo5Δ rad2Δ* strain compared to the wild-type and single mutants, suggesting that Exo5 and FEN1 are redundantly required for mitochondrial DNA maintenance (Fig. 2C). In several experiments, the abundance of mitochondrial DNA in *exo5Δ rad2Δ* varied between

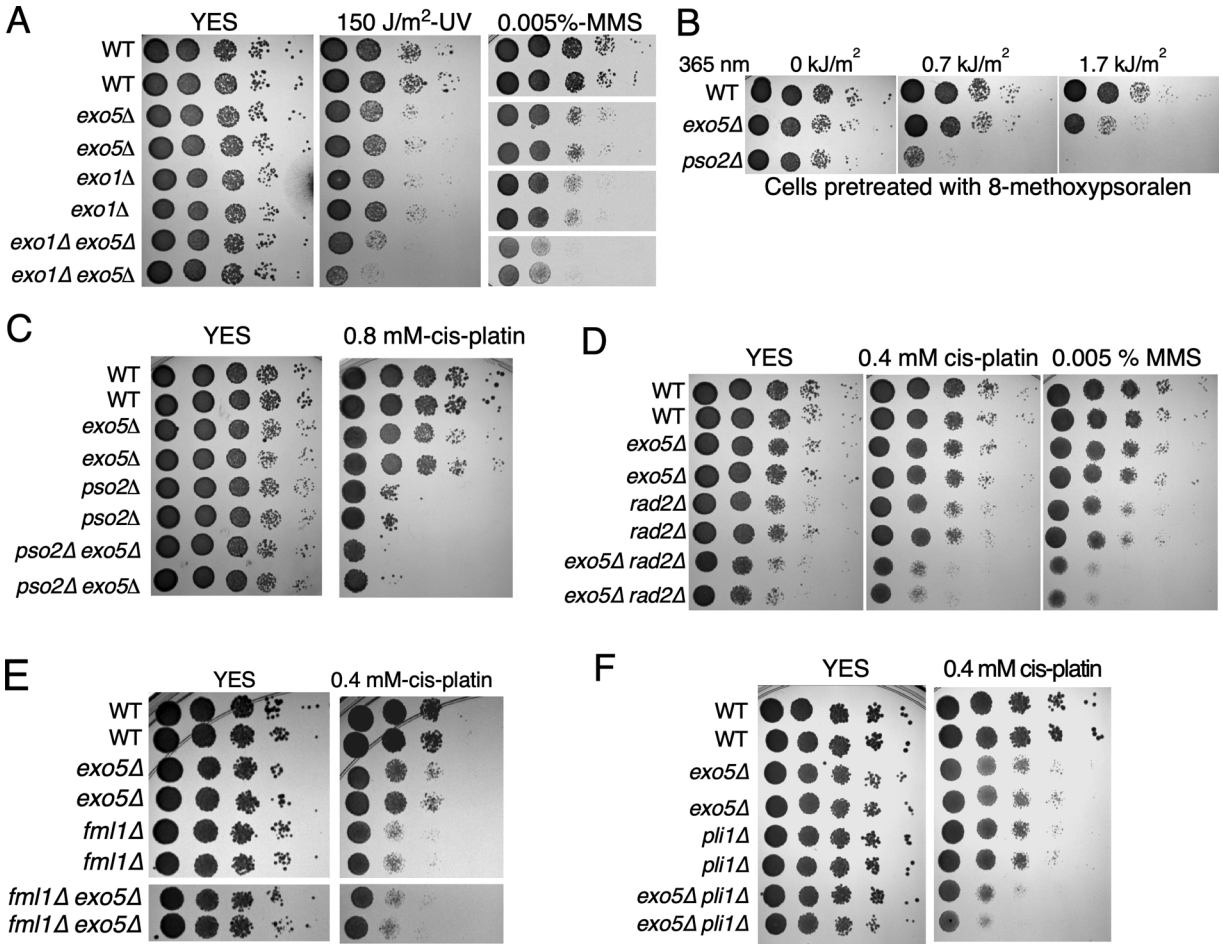

Fig. 5. Exo5 genetic interactions in DNA repair pathways. (A) Epistasis experiment with *exo1Δ*. Ten-fold serial dilutions were plated on YES plates and exposed to UV-irradiation, or plated on YES supplemented with the indicated concentration of MMS. Right panel was rearranged for presentation; the original is shown in Supplementary Fig. S3E. (B) Sensitivity to acute psoralen treatment as described in the methods. Cells were washed twice with PBS buffer and diluted for spotting on YES plates. (C) Epistasis experiment with *pso2Δ* for sensitivity to chronic cis-platin treatment as described in the methods. Cells were spotted in ten-fold dilutions. (D) Epistasis experiments with *rad2Δ* for sensitivity to chronic cis-platin and MMS. (E) Epistasis experiments with *fml1Δ* for sensitivity to chronic cis-platin. Selected sections are shown; the full figure is in Supplementary Fig. S4B. (F) Epistasis experiments with *pli1Δ* for sensitivity to chronic cis-platin.

5–15% that of wild-type. No specific deletions were detected by altering the restriction enzymes used to digest the circular mitochondrial genome, nor were they detected by carrying out PCR with a series of primer sets that covered the circular genome (data not shown). Furthermore, the mitochondrial DNA loss phenotype was complemented by introduction of wild-type *Exo5*$^{+}$ and of *exo5-(58-409)* on a plasmid, but not by the *exo5-M58A* mutant (Fig. 2D). These sets of data further support our model that the mitochondrial isoform of Exo5 results from initiation of translation at methionine-58. We conclude that those mitochondrial genomes that were defective due to the combined lack of FEN1 and Exo5 were lost from the population, perhaps by mitophagy [22]. The results from these experiments establish a redundant function in mitochondria for Exo5 and FEN1, presumably operating during the final steps of DNA replication in order to generate ligatable nicks.

3.5. Fission yeast Exo5 is important for DNA repair

In order to determine the possible participation of spExo5 in various nuclear DNA repair pathways, we carried out *in vivo* survival assays of *exo5Δ* mutant strains after exposure to DNA damaging agents. We detected no hypersensitivity of *exo5Δ* to γ-irradiation (Supplementary Fig. S4A), nor is a *mre11Δ* mutant, which is defective for X-ray repair, hypersensitized by the additional *exo5Δ* mutation (Supplementary Fig. 4B). However, the *exo5Δ* mutant is more sensitive than isogenic wild-type to UV-irradiation and alkylating agents (Fig. 5A). Furthermore, the deletion is particularly hypersensitive to interstrand crosslinking (ICL) agents such as 8-methoxypsoralen (Fig. 5B) and cis-platin (Fig. 5C). 8-methoxypsoralen intercalates into the DNA and forms interstrand crosslinks upon irradiation with visible light [23]. Remarkably, these results with DNA damaging agents recapitulate the knockdown experiments in human cells; hExo5-depleted cells showed hypersensitivity to UV, MMS, and cis-platin, but no hypersensitivity to γ-irradiation [3]. However, these phenotypes differ dramatically from those in *S. cerevisiae*, in which the *exo5Δ* mutant showed wild-type sensitivity to all DNA damaging agents tested, but was solely defective for mitochondrial DNA maintenance [2]. These damage-sensitivity phenotypes allowed us to use *S. pombe* as a tool to map genetic interactions between spExo5 and known components of various DNA repair pathways. We carried out DNA damage sensitivity experiments with a set of mutations in known DNA repair genes, with a particular focus on interstrand crosslink (ICL) repair pathways. The results of these epistasis experiments are shown in Fig. 5 in and Supplementary Figures S4 and S5.

The strongest *exo5Δ* phenotype was observed when the deletion was combined with *rad2Δ* (FEN1). In the nucleus, FEN1 nuclease is required for Okazaki fragment maturation, ribonucleotide excision repair, and long patch base-excision repair [24–26]. The *rad2Δ exo5Δ* double mutant showed a synthetic growth defect even in absence of DNA damage (Fig. 5D). As described above, this growth defect could be the result of the loss of respiratory fitness of the double mutant, which is caused by

severe loss of mitochondrial DNA (Fig. 2B,C). In addition, treatment of the *rad2Δ exo5Δ* strain with either MMS or cis-platin revealed strong hypersensitivity to these DNA damaging agents that is consistent with a synergistic interaction (Fig. 5D). Therefore, unless the loss of respiratory function sensitizes fission yeast to DNA damaging agents, these data indicate that Exo5 and FEN1 operate largely in different DNA repair pathways in the nucleus.

Fission yeast Exo1 exonuclease is involved in Okazaki fragment maturation, double-strand break repair, mismatch repair, and interstrand crosslink repair [27–29]. While the single *exo1Δ* and *exo5Δ* mutants showed a comparable sensitivity to UV, MMS and ICL agents, the double mutant *exo1Δ exo5Δ* showed an increased sensitivity to these agents, indicating that Exo1 and Exo5 repair these damages with partial redundancy (Fig. 5A, Supplementary Fig. S4E). However, the double mutant was not sensitive to γ-irradiation, again supporting a model in which Exo5 is not involved in double-strand break repair (Supplementary Fig. S4A). The UV sensitivity of a *rad13Δ* mutant, the 3′-endonuclease that functions in nucleotide excision repair (ortholog of human XPG) is increased in the double mutant with *exo5Δ*, suggesting that Exo5 does not have a function in nucleotide excision repair.

In *S. pombe*, there are three distinct, but partially redundant pathways for the repair of ICLs. One pathway has been established through the study of mutations in *fan1*$^+$, *fml1*$^+$, and *rad51*$^+$, involving the Fanconi genes together with homologous recombination [30,31]. A second pathway, acting in parallel with the Fanconi pathway, is defined by *pso2*$^+$ and requires the nucleotide excision repair factor *rad13*$^+$ (ortholog of human XPG) and homologous recombination (*rad51*$^+$) [32,33]. Thus, both the Fanconi and Pso2/nucleotide excision repair pathway also depend on homologous recombination. In addition, the SUMO E3 ligase *pli1*$^+$ is involved in the resolution of DNA crosslinks in a separate pathway [31]. Given the sensitivity of *exo5Δ* for ICL agents, we carried out an epistasis analysis to determine in what ICL repair pathway Exo5 may function. The crosslink sensitivity of *pso2Δ* is substantially higher than that of *exo5Δ* (Fig. 5B, C), while the double mutant *exo5Δ pso2Δ* shows an increased sensitivity to cis-platin (Fig. 5C, Supplementary Fig. S5B). The Fanconi branch of ICL repair is represented by *fml1*$^+$ and *fan1*$^+$. *Exo5*$^+$ is epistatic with *fml1*$^+$, i.e. the double mutant is not more sensitive than the single mutants (Fig. 5E). Likewise, the *exo5Δ fan1Δ* double mutant is not more sensitive than the single mutants (Supplementary Fig. S5A). These data suggest that Exo5 functions in the Fanconi pathway of ICL repair. In support of this conclusion are epistasis experiments with *pli1*$^+$, which defines the third pathway through sumoylation [31]. *Exo5Δ* and *pli1Δ* show synergistic interactions indicating that they operate in different, competing pathways (Fig. 5F). Altogether, these data are consistent with a model in which Exo5 is required for ICL repair by the Fanconi pathway.

3.6. Conclusions

Our studies of Exo5 in three distantly related organisms, i.e. human and budding yeast, and here fission yeast, shows the remarkable versatility of this exonuclease. Exo5 has revealed an essential mitochondrial function, but no nuclear function in budding yeast, an important nuclear function and a redundantly essential mitochondrial function in fission yeast, and an important nuclear function in human. The fact that the Exo5 gene has been lost several times during evolution, e.g. in some superorders of worms and birds, but not in others, and in all insects, might suggest that its absence would be easy to compensate for by other exonucleases (Supplementary Fig. 1). Yet, the strong correlation of several types of cancers with EXO5 silencing suggests that at least in humans this is not the case [5].

S. pombe has provided a genetic tool for investigating the role of Exo5 in DNA repair. The DNA damage sensitivity of an *exo5Δ* strain closely recapitulates the hExo5 knockdown experiments in human cells [3]. *Exo5Δ* and *rad2Δ* (FEN1) show synergistic interactions in both nuclear and mitochondrial DNA metabolism (Fig. 2, 5D). FEN1 is required for Okazaki fragment maturation, long patch base-excision repair, and ribonucleotide excision repair [24,26]. It is possible that, similarly to the exonuclease/helicase Dna2, Exo5 plays a redundant function in Okazaki fragment maturation when ssDNA flaps become bound by RPA and FEN1 is no longer able to act [34–37]. Exo5 and FEN1 also play an essential redundant function in the mitochondria in *S. pombe*. Both enzymes are single-strand specific exonucleases that may be required to remove single-strand DNA flaps during the termination of mitochondrial DNA replication. In addition, Exo1, another nuclease in the FEN1 family appears to perform complementary functions to Exo5 in the repair of UV damage and MMS damage (Fig. 5A).

Exo5Δ strains were particularly sensitive to interstrand cross-linking agents, such as cis-platin and 8-methyoxypsoralen. The repair of ICLs has been investigated in *S. pombe* [31]. These studies have started to delineate the pathways for repair of ICLs, but there are still many questions that need to be investigated. There are at least three pathways that have been identified in *S. pombe* for ICL repair. One of these pathways involves the nuclease Fan1 and the helicase Fml1, which are Fanconi anemia homologs; the second pathway is dependent on the nuclease Pso2 and the nucleotide excision repair endonuclease Rad13 (XPG); the third pathway requires the sumo ligase Pli1 [31]. Exo5 is epistatic with the proteins of the Fan1 dependent pathway of repair and is non-epistatic with the Pso2 nuclease and with Pli1 (Fig. 5C,E,F). Future studies will be required to determine the mechanistic function of Exo5 in ICL repair.

Author contributions

JLS and PMB designed the experiments and wrote the paper. CMS carried out protein purification, KJG did the cell biological studies, and BLY carried out strain design and verification. All authors contributed to the final version of the paper.

Acknowledgements

The authors thank Nick Rhind, Susan Forsburg, for providing plasmids, and Tim Lohman for a gift of reverse polarity oligonucleotides. The authors would also like to thank Nick Rhind, Susan Forsburg, Anthony Carr, Hiroshi Iwasaki, Lynda Groocock, Albert Pastink, Nancy Walworth, Daniel Teasley, Emily Higuchi, Michael Boddy, Randy Hyppa, Paul Russell, Toru Nakamura for providing *S. pombe* strains. The authors thank Hiroshi Iwasaki for providing Ssb1 antibodies used in this study. This work was supported in part by the US National Institutes of Health (GM118129 to P.B.).

Appendix A. Supplementary data

Supplementary material related to this article can be found, in the online version, at doi:https://doi.org/10.1016/j.dnarep.2019.102720.

References

[1] P.M.J. Burgers, G.A. Bauer, L. Tam, Exonuclease V from Saccharomyces cerevisiae. A 5′– -3′-deoxyribonuclease that produces dinucleotides in a sequential fashion, J. Biol. Chem. 263 (1988) 8099–8105.
[2] P.M. Burgers, C.M. Stith, B.L. Yoder, J.L. Sparks, Yeast exonuclease 5 is essential for mitochondrial genome maintenance, Mol. Cell. Biol. 30 (2010) 1457–1466.
[3] J.L. Sparks, R. Kumar, M. Singh, M.S. Wold, T.K. Pandita, P.M. Burgers, Human exonuclease 5 is a novel sliding exonuclease required for genome stability, J. Biol. Chem. 287 (2012) 42773–42783.
[4] B. Paumard-Hernandez, O. Calvete, L. Inglada Perez, H. Tejero, F. Al-Shahrour, G. Pita, A. Barroso, J. Carlos Trivino, M. Urioste, C. Valverde, E. Gonzalez Billalabeitia, V. Quiroga, J. Francisco Rodriguez Moreno, A. Fernandez Aramburo, C. Lopez, P. Maroto, J. Sastre, M. Jose Juan Fita, I. Duran, I. Lorenzo-Lorenzo, P. Iranzo, X. Garcia Del Muro, S. Ros, F. Zambrana, A. Maria Autran, J. Benitez, Whole exome sequencing identifies PLEC, EXO5 and DNAH7 as novel susceptibility genes in testicular cancer, Int. J. Cancer 143 (2018) 1954–1962.
[5] T.A. Knijnenburg, L. Wang, M.T. Zimmermann, N. Chambwe, G.F. Gao, A.D. Cherniack, H. Fan, H. Shen, G.P. Way, C.S. Greene, Y. Liu, R. Akbani, B. Feng, L.A. Donehower, C. Miller, Y. Shen, M. Karimi, H. Chen, P. Kim, P. Jia, E. Shinbrot,

S. Zhang, J. Liu, H. Hu, M.H. Bailey, C. Yau, D. Wolf, Z. Zhao, J.N. Weinstein, L. Li, L. Ding, G.B. Mills, P.W. Laird, D.A. Wheeler, I. Shmulevich, N. Cancer Genome Atlas Research, R.J. Monnat Jr., Y. Xiao, C. Wang, Genomic and molecular landscape of DNA damage repair deficiency across the cancer genome atlas, Cell Rep. 23 (2018) 239–254 e236.

[6] A. Matsuyama, R. Arai, Y. Yashiroda, A. Shirai, A. Kamata, S. Sekido, Y. Kobayashi, A. Hashimoto, M. Hamamoto, Y. Hiraoka, S. Horinouchi, M. Yoshida, ORFeome cloning and global analysis of protein localization in the fission yeast Schizosaccharomyces pombe, Nat. Biotechnol. 24 (2006) 841–847.

[7] N. Reynolds, E. Warbrick, P.A. Fantes, S.A. MacNeill, Essential interaction between the fission yeast DNA polymerase delta subunit Cdc27 and Pcn1 (PCNA) mediated through a C-terminal p21(Cip1)-like PCNA binding motif, EMBO J. 19 (2000) 1108–1118.

[8] J. Walker, P. Crowley, A.D. Moreman, J. Barrett, Biochemical properties of cloned glutathione S-transferases from Schistosoma mansoni and Schistosoma japonicum, Mol. Biochem. Parasitol. 61 (1993) 255–264.

[9] G.O. Bylund, J. Majka, P.M. Burgers, Overproduction and purification of RFC-related clamp loaders and PCNA-related clamps from Saccharomyces cerevisiae, Methods Enzymol 409 (2006) 1–11.

[10] S. Pokharel, J.L. Campbell, Cross talk between the nuclease and helicase activities of Dna2: role of an essential iron-sulfur cluster domain, Nucleic Acids Res. 40 (2012) 7821–7830.

[11] J.T. Yeeles, R. Cammack, M.S. Dillingham, An iron-sulfur cluster is essential for the binding of broken DNA by AddAB-type helicase-nucleases, J. Biol. Chem. 284 (2009) 7746–7755.

[12] A.V. Nimonkar, J. Genschel, E. Kinoshita, P. Polaczek, J.L. Campbell, C. Wyman, P. Modrich, S.C. Kowalczykowski, BLM-DNA2-RPA-MRN and EXO1-BLM-RPA-MRN constitute two DNA end resection machineries for human DNA break repair, Genes Dev. 25 (2011) 350–362.

[13] L. Kazak, A. Reyes, J. He, S.R. Wood, G. Brea-Calvo, T.T. Holen, I.J. Holt, A cryptic targeting signal creates a mitochondrial FEN1 isoform with tailed R-Loop binding properties, PLoS One 8 (2013) e62340.

[14] S.F. Pinter, S.D. Aubert, V.A. Zakian, The Schizosaccharomyces pombe Pfh1p DNA helicase is essential for the maintenance of nuclear and mitochondrial DNA, Mol. Cell. Biol. 28 (2008) 6594–6608.

[15] S.L. Forsburg, Comparison of Schizosaccharomyces pombe expression systems, Nucleic Acids Res. 21 (1993) 2955–2956.

[16] N. Haruta, Y. Kurokawa, Y. Murayama, Y. Akamatsu, S. Unzai, Y. Tsutsui, H. Iwasaki, The Swi5-Sfr1 complex stimulates Rhp51/Rad51- and Dmc1-mediated DNA strand exchange in vitro, Nat. Struct. Mol. Biol. 13 (2006) 823–830.

[17] G. Jimenez, J. Yucel, R. Rowley, S. Subramani, The rad3+ gene of Schizosaccharomyces pombe is involved in multiple checkpoint functions and in DNA repair, Proc. Natl. Acad. Sci. U. S. A. 89 (1992) 4952–4956.

[18] A.M. Carr, Control of cell cycle arrest by the Mec1sc/Rad3sp DNA structure checkpoint pathway, Curr. Opin. Genet. Dev. 7 (1997) 93–98.

[19] P. Haffter, T.D. Fox, Nuclear mutations in the petite-negative yeast Schizosaccharomyces pombe allow growth of cells lacking mitochondrial DNA, Genetics 131 (1992) 255–260.

[20] L. Kalifa, G. Beutner, N. Phadnis, S.S. Sheu, E.A. Sia, Evidence for a role of FEN1 in maintaining mitochondrial DNA integrity, DNA Repair (Amst) 8 (2009) 1242–1249.

[21] P. Liu, L. Qian, J.S. Sung, N.C. de Souza-Pinto, L. Zheng, D.F. Bogenhagen, V.A. Bohr, D.M. Wilson 3rd, B. Shen, B. Demple, Removal of oxidative DNA damage via FEN1-dependent long-patch base excision repair in human cell mitochondria, Mol. Cell. Biol. 28 (2008) 4975–4987.

[22] T. Kanki, K. Furukawa, S. Yamashita, Mitophagy in yeast: Molecular mechanisms and physiological role, Biochim. Biophys. Acta 1853 (2015) 2756–2765.

[23] R.S. Cole, Psoralen monoadducts and interstrand cross-links in DNA, Biochim. Biophys. Acta 254 (1971) 30–39.

[24] Y. Liu, H.I. Kao, R.A. Bambara, Flap endonuclease 1: a central component of DNA metabolism, Annu. Rev. Biochem. 73 (2004) 589–615.

[25] P.M.J. Burgers, T.A. Kunkel, Eukaryotic DNA replication fork, Annu. Rev. Biochem. 86 (2017) 417–438.

[26] J.L. Sparks, H. Chon, S.M. Cerritelli, T.A. Kunkel, E. Johansson, R.J. Crouch, P.M. Burgers, RNase H2-initiated ribonucleotide excision repair, Mol. Cell 47 (2012) 980–986.

[27] P.T. Tran, N. Erdeniz, L.S. Symington, R.M. Liskay, EXO1-A multi-tasking eukaryotic nuclease, DNA Repair (Amst) 3 (2004) 1549–1559.

[28] L.J. Barber, T.A. Ward, J.A. Hartley, P.J. McHugh, DNA interstrand cross-link repair in the Saccharomyces cerevisiae cell cycle: overlapping roles for PSO2 (SNM1) with MutS factors and EXO1 during S phase, Mol. Cell. Biol. 25 (2005) 2297–2309.

[29] E.P. Mimitou, L.S. Symington, DNA end resection: many nucleases make light work, DNA Repair (Amst) 8 (2009) 983–995.

[30] W. Sun, S. Nandi, F. Osman, J.S. Ahn, J. Jakovleska, A. Lorenz, M.C. Whitby, The FANCM ortholog Fml1 promotes recombination at stalled replication forks and limits crossing over during DNA double-strand break repair, Mol. Cell 32 (2008) 118–128.

[31] Y. Fontebasso, T.J. Etheridge, A.W. Oliver, J.M. Murray, A.M. Carr, The conserved Fanconi anemia nuclease Fan1 and the SUMO E3 ligase Pli1 act in two novel Pso2-independent pathways of DNA interstrand crosslink repair in yeast, DNA Repair (Amst) 12 (2013) 1011–1023.

[32] L.M. Groocock, J. Prudden, J.J. Perry, M.N. Boddy, The RecQ4 orthologue Hrq1 is critical for DNA interstrand cross-link repair and genome stability in fission yeast, Mol. Cell. Biol. 32 (2012) 276–287.

[33] S. Lambert, S.J. Mason, L.J. Barber, J.A. Hartley, J.A. Pearce, A.M. Carr, P.J. McHugh, Schizosaccharomyces pombe checkpoint response to DNA interstrand cross-links, Mol. Cell. Biol. 23 (2003) 4728–4737.

[34] R.S. Murante, L. Rust, R.A. Bambara, Calf 5′ to 3′ exo/endonuclease must slide from a 5′ end of the substrate to perform structure-specific cleavage, J. Biol. Chem. 270 (1995) 30377–30383.

[35] S.H. Bae, K.H. Bae, J.A. Kim, Y.S. Seo, RPA governs endonuclease switching during processing of Okazaki fragments in eukaryotes, Nature 412 (2001) 456–461.

[36] R. Ayyagari, X.V. Gomes, D.A. Gordenin, P.M. Burgers, Okazaki fragment maturation in yeast. I. Distribution of functions between FEN1 AND DNA2, J. Biol. Chem. 278 (2003) 1618–1625.

[37] H.I. Kao, J. Veeraraghavan, P. Polaczek, J.L. Campbell, R.A. Bambara, On the roles of Saccharomyces cerevisiae Dna2p and Flap endonuclease 1 in Okazaki fragment processing, J. Biol. Chem. 279 (2004) 15014–15024.

Supplementary Information to:

The roles of fission yeast Exonuclease 5 in nuclear and mitochondrial genome stability

Justin L. Sparks[1,2], Kimberly J. Gerik[1], Carrie M. Stith[1], Bonita L. Yoder[1], and Peter M. Burgers[1*]

[1]Department of Biochemistry and Molecular Biophysics, Washington University School of Medicine, St. Louis, MO 63110, USA; [2]Department of Biological Chemistry and Molecular Pharmacology, Harvard Medical School, Boston, MA 02115, USA
*Corresponding author: TEL (314) 362-3772; FAX (314) 362-7183; burgers@wustl.edu

Supplementary Table 1. *S. pombe* strains used.

Strain	Relevant mutations	Genotype	Source
JY746	Wild-type	h+ ura4-D18 leu1-32 ade6-M210	Hiroshi Iwasaki
NBY2027	rad51Δ	h- ura4-D18 leu1-32 rad51::ura4	Paul Russell
1008	rad2Δ	h+ rad2::hphMX6 ade6-M216 his3-D1 leu1-32 ura4-D18	Sheila Stewart
GP6928	rad32Δ	h- ade6-52 ura4-D18 rad32::ura4	Gerald Smith
SAL181	pso2Δ	h- ade6-704 leu1-32 pso2::kanMX6 ura4-D18	A. M. Carr
GP5860	Wild-type	h- ade6-D19 ura4-D18 leu1-32 his3-D1	Gerald Smith
Y3	Wild-type	h- ade6-M210 leu1-32 ura4-D18	Shinji Yasuhira
Y19	rad13Δ	h- ade6-M210 leu1-32 ura4-D18 rad13::ura4	Shinji Yasuhira
OL4175	exo1Δ	h- leu1-32 ura4-D18 exo1::ura4	Paul Russell
CF15	Wild-type	h- leu1-32 ura4-D18 ade6-M210 his3-D1	Nakamura
TN1374	rad3Δ	h- leu1-32 ura4-D18 ade6-M210 his3-D1 rad3::LEU2	Nakamura
MCW2080	fml1Δ	h+ fml1::natMX4 ura4-D18 his3-D1 leu1-32 arg3-D4	Matthew Whitby
PYP100	exo5Δ	h+/h+ ade6-M210/ade6-M216 ura4-D18/ura4-D18 leu1-32/leu1-32 exo5::kanMX6	Bioneer
PYP101	Wild-type	h- leu1-32 ura4-D18 ade6-M210 his3-D1	This study
PYP102	exo5Δ	h+ ade6-M210 leu1-32 ura4-D18 exo5::kanMX6 his3-D1	This study
PYP103	fan1Δ	h- leu1-32 ura4-D18 ade6-M210 his3-D1 fan1::hphMX6	This study
PYP104	pli1Δ	h- leu1-32 ura4-D18 ade6-M210 his3-D1 pli1::hphMX6	This study
PYP105	exo5Δ exo1Δ	h+ ade6-M210 leu1-32 ura4-D18 exo5::kanMX6 exo1::ura4+	This study
PYP106	exo5Δ pso2Δ	h+ ade6-M210 leu1-32 ura4-D18 exo5::kanMX6 pso2::kanMX6	This study
PYP107	rad13Δ exo5Δ	h- ade6-M210 leu1-32 ura4-D18 rad13:: ura4+ exo5::kanMX6	This study
PYP109	rad32Δ exo5Δ	h- ade6-M210 ura4-D18 rad32::ura4+ exo5::kanMX6	This study
PYP110	rad2Δ exo5Δ	h+ ade6-M210 leu1-32 ura4-D18 rad2::hphMX4 exo5::kanMX6	This study
PYP115	exo5Δ fan1Δ	h+ ade6-M210 leu1-32 ura4-D18 exo5::kanMX6 fan1::hphMX6	This study
PYP116	exo5Δ pli1Δ	h+ ade6-M210 leu1-32 ura4-D18 exo5::kanMX6 pli1::hphMX6	This study
PYP117	exo5Δ fml1Δ	h+ fml1::natMX4 ura4-D18 his3-D1 leu1-32 arg3-D4 exo5::kanMX6	This study
PYP142	exo5Δ rad51	h- leu1-32 ura4-D18 ade6-M210 his3-D1 rad51::ura4 exo5::kanMX6	This study
PYP174	rad2Δ	h- leu1-32 ura4-D18 ade6-M210 his3-D1 rad2::hphMX6	This study
PYP175	rad2Δ exo5Δ	h- leu1-32 ura4-D18 ade6-M210 his3-D1 rad2::hphMX6 exo5::kanMx6	This study

Supplementary Table 2. Exo5 localization. The *exo5Δ* mutant strain PYP102, containing the indicated forms of *exo5*, together with a C-terminal fusion to GFP (plasmids pBL289 series), were grown in EMM selective media in the presence of 5 μM thiamine, and processed for fluorescence microcopy basically as described [1]. Cells were spun down and suspended in 1 mL buffered glucose [100 mM HEPES-NaOH pH 7.7 + 2% glucose] plus 20 ug/mL Hoechst 33342 (Invitrogen/Molecular Probes) DNA dye and incubated in a roller drum at 30ºC for 20 minutes. Cells were fixed by the addition of 100 μl 37% formaldehyde and incubated in a roller drum at 30ºC for 5 additional minutes. Cells were harvested by centrifugation for 30 seconds at 4,000 x *g* and washed twice with 0.5 ml of buffered glucose; they were suspended in 50 μl buffered glucose and 2-3 μl were viewed at 1,000X magnification using oil on an Olympus AHBT3 microscope (Gfp excitation/emission = 395/509 nm; Hoechst 33342 excitation/emission = 350/461 nm). The Invitrogen/Molecular Probes protocol was used with MitoTracker Orange M7510. Quantification is shown below.

Cells containing wild-type Exo5-GFP (top left) show pan-cytoplasmic and nuclear GFP fluorescence. The punctate cytoplasmic GFP fluorescence is consistent with mitochondrial localization. Cells that are in addition co-stained with MitoTracker show colocalization of cytoplasmic GFP and MitoTracker (top right). Cells containing the M58A mutant of Exo5-GFP (bottom left) show diffuse cytoplasmic and nuclear staining. The punctate cytoplasmic staining, observed in wild-type cells, is largely absent from these mutant cells, suggesting that the M58A-Exo5 does not localize to mitochondria. Additional MitoTracker staining (bottom right) does not show co-localization of GFP with punctate MitoTracker staining. Cells containing the Δ(1-57) truncation form of Exo5-GFP (middle right) show exclusively punctate cytoplasmic fluorescence, consistent with mitochondrial localization. GFP is excluded from the nucleus. Unfortunately, for the Exo5-Δ(1-57)-GFP cells, MitoTracker staining was very poor, and there were no cells that showed both MitoTracker and GFP fluorescence.

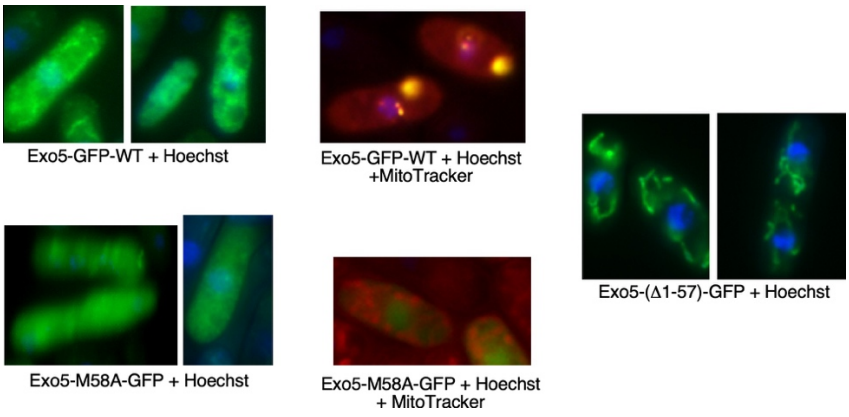

exo5	**%Nuclear**	**% mito**	**% nuclear+mito**
wild-type (N=37)	39	43	18
M58A (N=32)	56	22	22
Δ(1-57) (N= 31)	0	100	0

Supplementary Table 3. Mass spectrometry fingerprint of Exo5 Co-IP. Results acquired from co-immunopurification of spExo5-3XFLAG interacting proteins in Figure 3A.

MASCOT Score	Protein Name	MW	% Coverage
Upper Sector			
616	Exo5	48365	53.3
412	single-stranded DNA binding protein Ssb1	68154	41.1
123	AAA family ATPase Rvb1	50021	12.1
102	AAA family ATPase Rvb2	51529	22.4
86	AAA family ATPase Cdc48	90069	8.8
42	single-stranded telomeric binding protein Tgc1	37980	16.9
25	TFIIH regulator Mms19	114597	0.9
21	crm1-N1 protein	123650	0.7
Lower Sector			
1000	Exo5	48365	54.3
266	14-3-3 protein Rad24	30357	29.5
190	14-3-3 protein Rad25	30350	24.4
174	PCNA	28951	42.7
160	single-stranded DNA binding protein Ssb2	30372	45.5
71	Rim1	17129	25.3

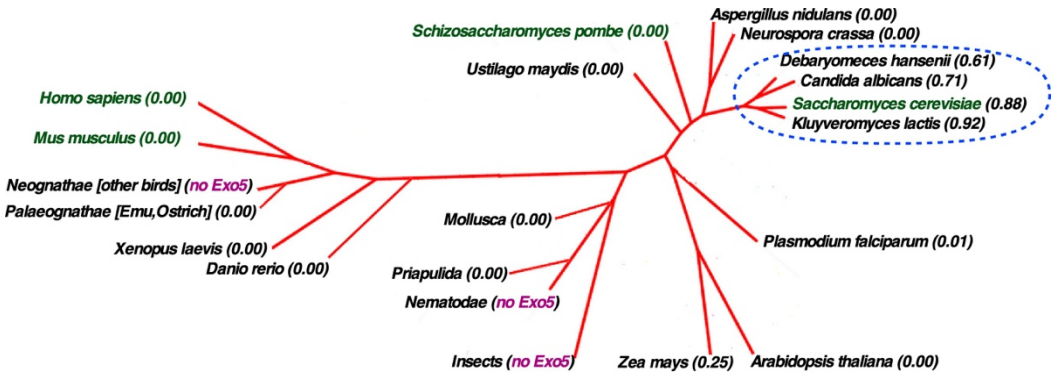

Supplementary Figure 1. Phylogenetic analysis of Exo 5. Shown is an unrooted phylogenetic tree of several model organisms and orders/superorders (generated at iTOL2.embl.de). In green are the forms of Exo5 studied in this and in previous publications. Numbers in brackets after the name are **Predotar** probability predictions of putative mitochondrial targeting for Methionine-1 in the ORF (urgi.versailles.inra.fr/predotar). In purple (no Exo5), no putative Exo5 gene was found for this order/superorder in the genome database by standard PSI-Blast analysis. Circled in blue are species in the *Saccharomycetales* family of fungi.

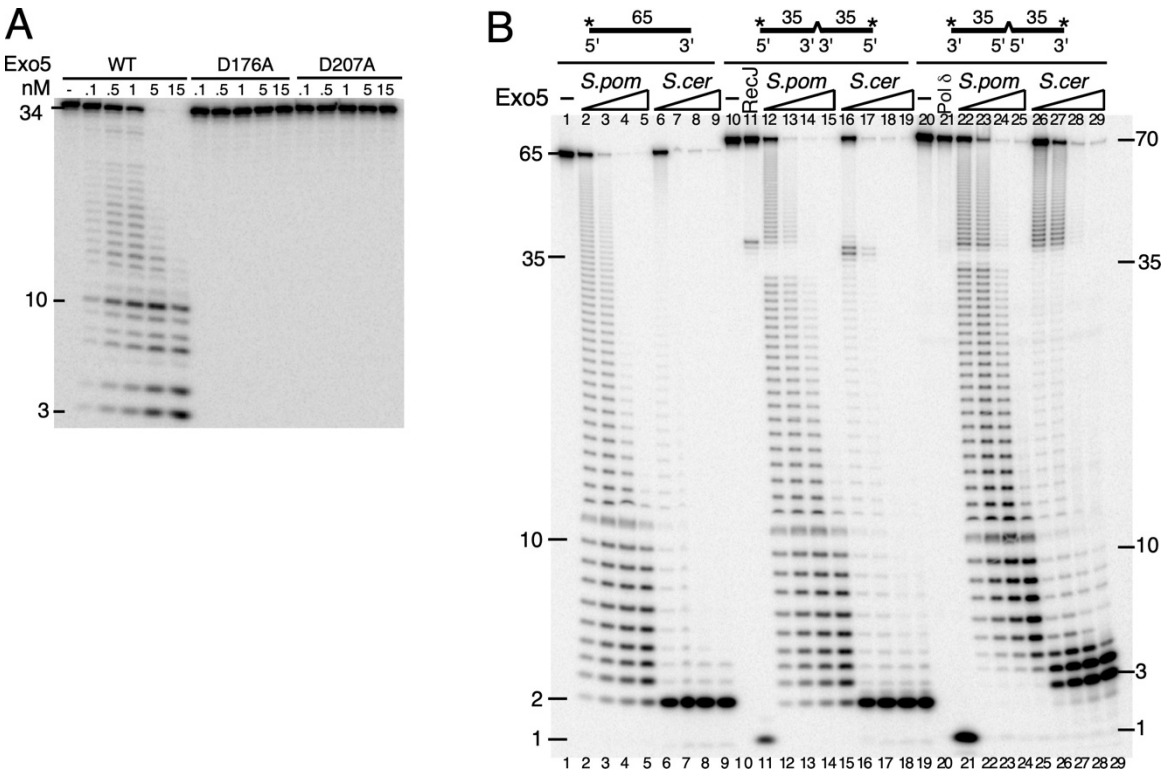

Supplementary Figure 2. Activity of *S. pombe* Exo5. (A) The indicated concentrations of Exo5 or mutant Exo5 were assayed on the labeled linear 34-mer, as shown in Fig. 1D, under standard assay conditions. D176 and D207 are the conserved aspartates essential for metal ion binding (see Fig. 1A). (B) Comparison of activity of *S. pombe* and *S. cerevisiae* Exo5 on polarity-switch oligonucleotides. Standard assays contained 10nM of either 5'-labeled $(dT)_{65}$, or 5'-labeled 5'-5'-ended $(dT)_{70}$, or 3'-labeled (with terminal transferase and α-^{32}P-dTTP) 3'-3'-ended $(dT)_{70}$. Incubation was for 4 min at 30˚C with either 0.15, 0.5, 1, or 5 nM of spExo5 or 0.05, 0.15, 0.5, or 1.0 nM nM of scExo5. Positive controls contained RecJ (a 5'-exonuclease) for the 5'-5-ended DNA and (lane 11) and DNA polymerase δ (Polδ) for the 3'-3'-ended DNA (lane 21). Samples were analyzed on 7 M urea-18% polyacrylamide gels and quantified by phosphorimaging. The *asterisks* indicate the position of the ^{32}P label. Note that scExo5 shows strict dinucleotide cleavage specificity when cutting from the 5'-ends (lanes 6-9 and 16-19), but cleaves 3-5 mers when cutting from the 3'-ends (lanes 26-29). As guidance for this crooked gel, lane numbers are given both at top and bottom.

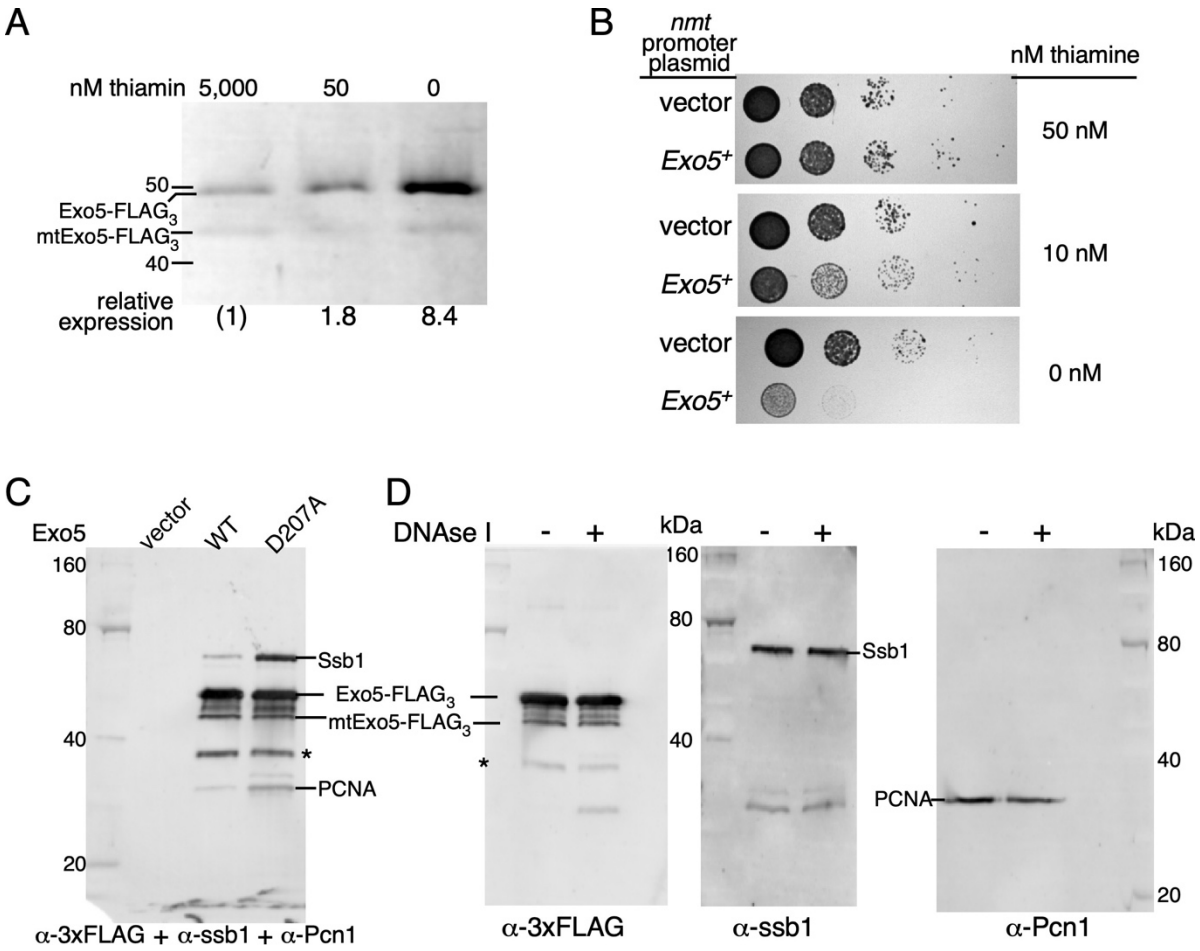

Supplementary Figure 3. SpExo5 expression analysis and immunoblots. (A) Strain PYP102 containing plasmid pBL289 with *exo5*-FLAG$_3$ under control of the *nmt* promoter, was grown in MME media with indicated concentrations of thiamine. Extracts were subjected to immunoblot analysis with 3xFLAG antibodies. Positions of full-length Exo5-FLAG$_3$ and the putative mitochondrial form (see Fig. 2A) are indicated. (B) Strain PYP102 containing empty vector or plasmid pBL288 with *Exo5*$^+$ under control of the *nmt* promoter was plated on EMM selective media with indicated concentrations of thiamine. (C,D) These are the full Western blot analyses associated with Figure 3 data. Positions of full-length Exo5-FLAG$_3$ and the putative mitochondrial form (see Fig. 2A) are indicated. Bands indicated with * are FLAG antibody-specific and may represent proteolytic fragments of Exo5-FLAG. (C) Western analysis of co-immunopurifications of extracts from *exo5Δ* cells containing either empty vector, or plasmids containing 3xFLAG-Exo5 or the nuclease-defective 3xFLAG-spExo5-D207A mutant. Rabbit antibodies against 3xFLAG (spExo5-FLAG), spSsb1 (RPA70 subunit), and spPcn1 (PCNA) were used in a cocktail. Select sections of the blot were used in Figure 2B. (D) Western analysis with separate antibodies as indicated, of extracts as in (A), either mock-treated or treated with DNaseI. Select sections of the blot were used in Figure 2C.

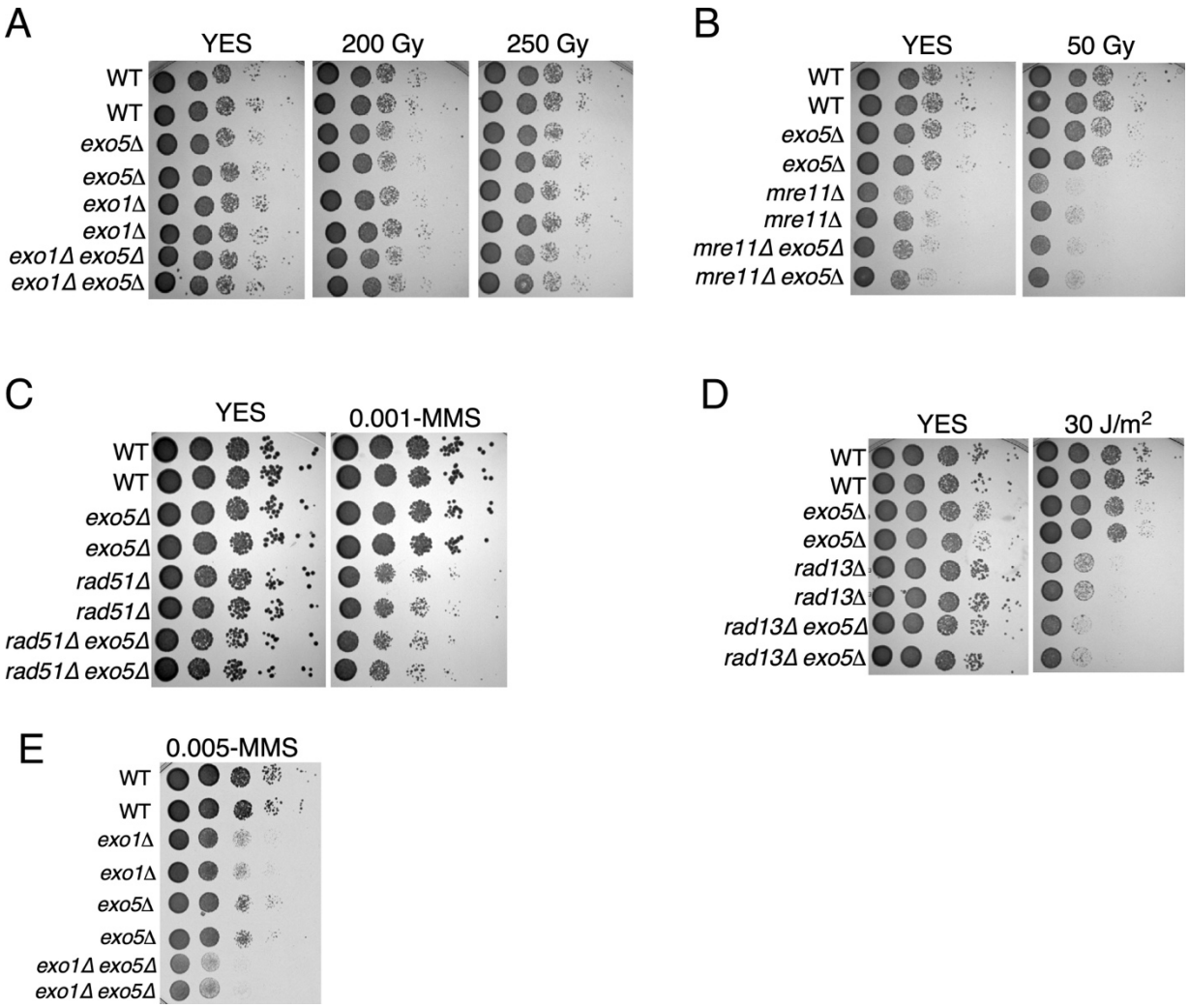

Supplementary Figure 4. Epistasis analysis. (A) Epistasis experiment using *exo5*Δ and *exo1*Δ for sensitivity to ionizing radiation. (B) Epistasis experiment using *exo5*Δ and *mre11*Δ for sensitivity to ionizing radiation. (C) Epistasis experiment using *exo5*Δ and *rad51*Δ for sensitivity to MMS. (D) Epistasis experiment using *exo5*Δ and *rad13*Δ for sensitivity to ionizing UV-irradiation. (E) Original figure for the epistasis analysis shown in Figure 5A, right panel.

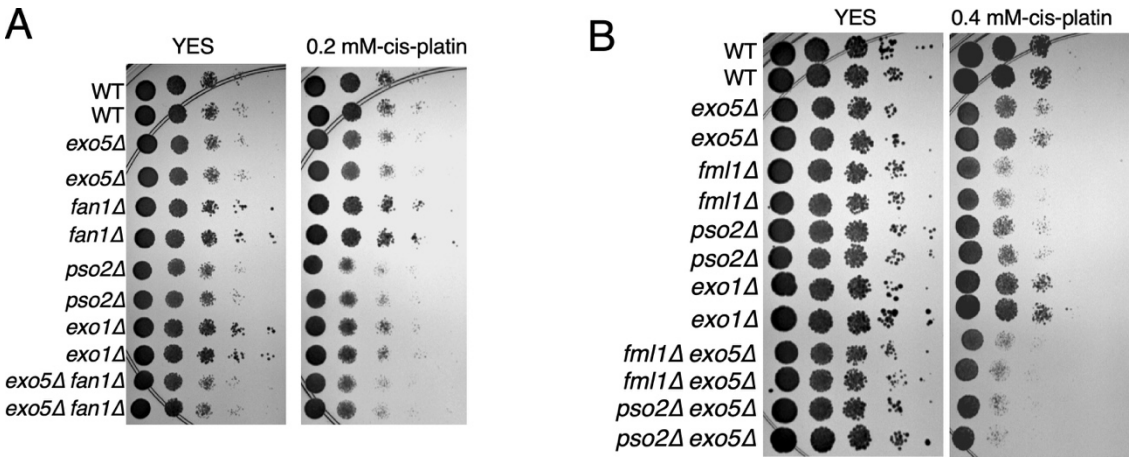

Supplementary Figure 5. SpExo5 is Epistatic with the Fan1 pathway and non-epistatic with Pso2. (A) Epistasis experiment using *exo5*Δ, *fan1*Δ, *pso2*Δ, *exo1*Δ testing sensitivity to chronic cis-platin treatment. (B) Epistasis experiment using *exo5*Δ, *exo1*Δ, *fml1*Δ, *pso2*Δ, testing sensitivity to chronic cis-platin treatment.

Supplementary reference

[1] I.M. Hagan, K.R. Ayscough, Fluorescence microscopy in yeast, in: V.J. Allan (Ed.) Protein localization by fluorescence microscopy, Oxford University Press, New York, NY, 2000, pp. 179-206.